



ELSEVIER

Journal of Physics and Chemistry of Solids 62 (2001) 1023–1037

JOURNAL OF  
PHYSICS AND CHEMISTRY  
OF SOLIDS

www.elsevier.nl/locate/jpcs

# Chemical state of a supported iron–cobalt catalyst during co disproportionation

## II. Experimental study

J.P. Pinheiro<sup>a</sup>, P. Gadelle<sup>a,\*</sup>, C. Jeandey<sup>b</sup>, J.L. Oddou<sup>b</sup>

<sup>a</sup>Laboratoire de Thermodynamique et Physico-Chimie Métallurgiques, CNRS-INPG-UJF, Ecole Nationale Supérieure d'Electrochimie et d'Electrometallurgie de Grenoble, BP 7538402, Saint Martin d'Hères, France

<sup>b</sup>Laboratoire de Chimie de Coordination Unité de Recherche Associée UJF-CNRS no. 1194 Service de Chimie Inorganique et Biologique, Département de Recherche Fondamentale sur la Matière Condensée CEA38054 Grenoble Cedex 9, France

Received 28 January 2000; accepted 10 October 2000

### Abstract

X-ray diffraction and Mössbauer spectroscopy have been used to investigate the chemical state of a supported iron–cobalt catalyst during the disproportionation of carbon monoxide at 800 K. The results of this study have demonstrated a strong implication of cementite Fe<sub>3</sub>C (may be in association with a cobalt carbide) in the alloy deactivation process. The deactivation due to the carburization is apparently reversible. The catalyst was, indeed, shown to partially recover its activity when submitted to conditions under which the carbide formation was not thermodynamically possible. The results of this study seem to indicate, however, that the alloy deactivation is not the consequence of a single phenomenon but results from the conjunction of two distinct processes. Additional deactivation due to the formation of a carbon layer at the particles surface appears as the most plausible hypothesis to explain this result. © 2001 Elsevier Science Ltd. All rights reserved.

**Keywords:** A. Alloys; B. Chemical synthesis; B. Vapor deposition; C. X-ray diffraction; C. Mössbauer spectroscopy

### 1. Introduction

The great variety of carbon materials that may be produced by catalytic decomposition of hydrocarbons constitutes probably one of the great interests of this method. Structures as different as filaments [1,2], nanotubes [3–5] or platelets [6] can, indeed, be produced by applying convenient reaction conditions. Although the fundamental reasons for this diversity are not still understood, it seems conceivable that, in the future, the morphology of the carbon deposit could be designed in function of the required application.

Independently of the nature of the catalyst itself, many parameters have been shown to have an influence on the morphology of the carbon deposit. Many strategies can therefore be imagined to produce carbon materials with an

adequate conformation. A direct way consists in acting on the composition of the gas mixture in contact with the catalyst. Nolan et al. [7] have demonstrated, for instance, that the addition of hydrogen to a CO–CO<sub>2</sub> mixture resulted in a radical change of the microstructure of the carbon deposit produced by reaction over a nickel catalyst. Nolan observed, indeed, that only nanotubes formed in the absence of hydrogen while, on the other hand, only carbon filaments were produced when hydrogen was introduced in the gas mixture. We observed the same phenomena over a cobalt catalyst [8]. Alloying constitutes also an easy way to modify both the catalyst activity and the morphology of the carbon deposit. Chambers et al. [9] have observed, for instance, that the addition of small amounts of copper to a cobalt catalyst was sufficient to produce a great increase of its activity towards ethylene decomposition. The structure of the carbon deposit was shown besides to differ greatly whether the reaction was carried out with a cobalt or a cobalt–copper catalyst.

The Fe<sub>50</sub>Co<sub>50</sub> (wt%) alloy is an efficient catalyst for the carbon filament growth when reacted with CO–CO<sub>2</sub>

\* Corresponding author. Tel.: +33-76-82-65-42; fax: +33-76-82-66-77.

E-mail address: p.gadelle@ltpcm.inpg.fr (P. Gadelle).

mixtures at temperature ranging from 723 to 873 K. In a previous paper [10], the results of a kinetic study performed at 800 K were briefly presented. This study demonstrated that the evolution of the reaction rate vs time was strongly depending on the composition of the gas mixture. In order to understand the origin of this phenomenon, thermodynamics was used to predict the possible transformations of this catalyst when contacted with CO–CO<sub>2</sub> mixtures. The aim of the present study is to compare these thermodynamical predictions with the experimental results. A special effort was also made to understand the deactivation mechanism of this alloy.

Experiments were carried out at 800 K on a Fe50 Co50 (wt%) catalyst with CO percentages ranging from 25 to 100%. Characterization of the catalyst after reaction was performed by a combination of Mössbauer spectroscopy and X-ray diffraction. Special care was taken to protect post-reaction samples from any contact with air.

## 2. Experimental process

The Fe50 Co50 (wt%) catalyst was prepared by incipient wetness impregnation of alumino-silicate fibers (Nextel®) with a solution of ethanol containing a mixture of iron and cobalt nitrates. The nitrate amounts to be dissolved in ethanol were adjusted in order to give, after appropriate treatment, a nominal metal content of about 10%. The impregnated samples were then dried in air at 353 K for 20 h before further treatment. Experiments were carried out in a small-sized flow reactor system operated at atmospheric pressure. Samples were pyrolyzed for 1 h under an helium flow at 523 K. After heating of the furnace to 800 K, helium was replaced by an H<sub>2</sub>/Ar (5/95) mixture and the catalysts were reduced for 16 h. After the reduction step, the reactor was flushed with helium for at least 4 h at the same temperature in order to remove any residual hydrogen. The catalysts were, then, reacted with CO–CO<sub>2</sub>. On-line chromatographic analyses of the gas mixture during the reaction, both at the inlet and outlet of the reactor, allowed computation of the reaction rate. It must be noticed that, in any case, an ultra pure CO was used in order to avoid impurities that could affect the results.

The reaction was stopped by flushing the reactor with helium and quenching it to room temperature. Owing to its small dimensions, the reactor could be introduced in a glove box. The X-ray diffraction and Mössbauer samples were, by this way, prepared without any contact with air. The whole post reaction sample was crushed and a part of the resulting powder was characterized without additional treatment using X-ray diffraction under controlled atmosphere ( $\lambda = 1.5406 \text{ \AA}$ ). The rest of the crushed sample was immersed in a Torr Seal® resin since Mössbauer studies were performed under ambient atmosphere.

The Mössbauer spectroscopy is an analysis technique specially well suited for compounds containing iron. It

permits particularly to obtain information on the chemical state of the iron atoms. <sup>57</sup>Fe Mössbauer measurements were generally performed at room temperature. The source was <sup>57</sup>Co in a rhodium matrix, moved in a sinusoidal mode with a maximum velocity calibrated at 12 mm s<sup>-1</sup>. The 14.4 keV  $\gamma$ -rays were detected by means of a proportional counter and Mössbauer spectra recorded on a 512 multichannel analyzer [11]. The spectra were analyzed in a least-square procedure by full diagonalization of the Hamiltonian describing the quadrupolar and magnetic interactions.

A blank analysis of the Torr Seal® resin demonstrated that its contribution to the global Mössbauer spectrum was not nil. As no iron compound was mentioned in the resin formula, we attributed this absorption signal to an iron-bearing impurity. The contribution of the resin to the whole spectrum was, however, shown to be generally minor in comparison with the contribution of the other phases and did not perturb their identification.

## 3. State of the catalyst before the reaction

Magnetic measurements on the supported catalyst after reduction were carried out by S. Herreyre [12]. This study demonstrated that the saturation magnetization of the catalyst was lying between 193 and 210 uem cgs g<sup>-1</sup> (1 uem cgs g<sup>-1</sup> = 1 A m<sup>2</sup> kg<sup>-1</sup>). This value is higher than half the sum of the saturation magnetization of the pure metals, which seems to demonstrate that iron and cobalt are not only coexisting as separated phases but are really alloyed.

This hypothesis is corroborated by other results.

The diffraction diagram of the reduced catalyst exhibits two lines whose position is close to those expected for the Fe50, Co50 (wt%) alloy (the iron–cobalt alloy is known to exhibit peaks whose position is close to that of fcc-iron). It is noteworthy that no line attributable either to hcp or fcc-cobalt is observed. For information, the position and the relative intensity of the different peaks related to iron or cobalt phases are indicated in the experimental diffraction diagram (Fig. 1).

The experimentally-determined cell parameter (2.8506 Å) is lower than the value which can be extrapolated from Ellis and Greiner's data (2.8570 Å) [13,14] and is closer to the value expected for an alloy with approximate mass composition Fe41, Co59 (wt%). This would imply that 30.5% of the iron atoms are not alloyed with cobalt. The hypothesis of two separated phases is, however, contradicted by the diffraction diagram. This one does not exhibit any peak besides those due to the Nextel® and those we attributed to the alloy. The latter are symmetrical. It is therefore implausible that they result from the superposition of two peaks, one due to the alloy and the other to isolated iron particles. Consistently, an average crystallite diameter of 20–30 nm was estimated from the broadening of the X-ray lines, values which are in good agreement with the direct

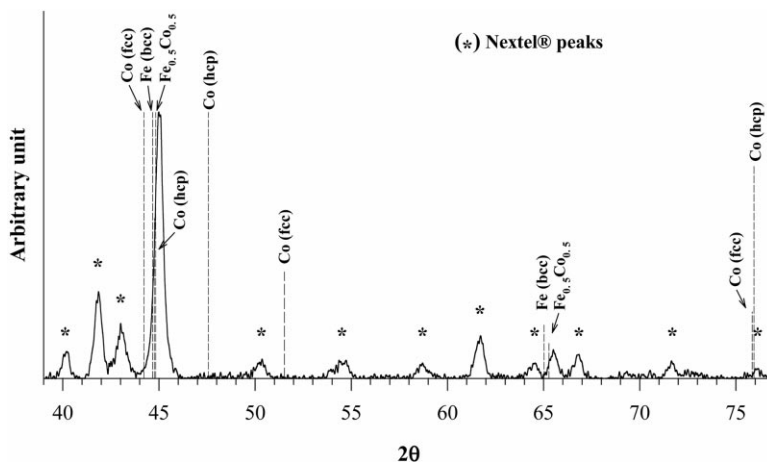


Fig. 1. Diffraction diagram of the reduced iron–cobalt catalyst ( $\lambda = 1.5406 \text{ \AA}$ ).

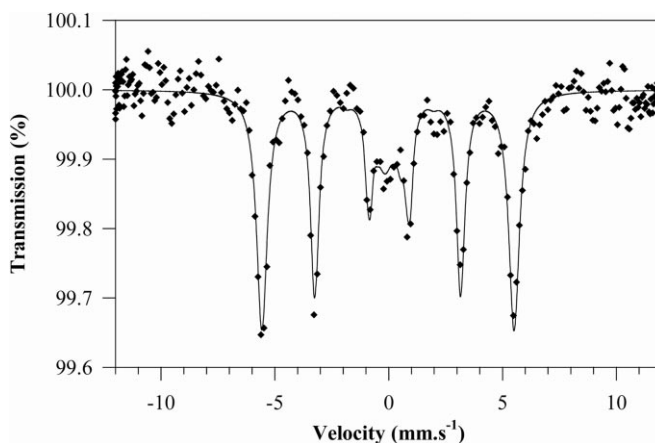


Fig. 2. Mössbauer spectrum of the reduced iron–cobalt catalyst.

measurements performed on M.E.T. The hypothesis of superposed peaks can therefore be ruled out.

The difference with Ellis and Greiner's results may, in our opinion, rather be attributed to the small size of the catalyst particles. Several authors [15,16] have, indeed, reported variations of the cell unit size occurring when the dimension of the particles is lowered to nanometric scale. These variations are generally assumed to result from modifications of the cohesive forces when the number of atoms decays under 100 in any direction of space.

The Mössbauer analysis of the reduced catalyst provided additional information (Fig. 2). The hyperfine field of the Fe50, Co50 (wt%) alloy is not known accurately: according to Johnson et al. [17], it would be between 346 and 355 kOe (1 Oe = 0.1 T). The value determined in the present work (344 kOe) is roughly in agreement with these values. The absence of peak corresponding to oxides, as previously in the diffraction diagram, seems to confirm the efficiency of

the precautions taken to avoid any contact of the samples with air. The Mössbauer spectrum of the reduced catalyst is characterized by relatively large absorption lines around  $0.38 \text{ mm s}^{-1}$ . This feature generally indicates the existence of a distribution of hyperfine fields inside the sample which would be the sign, in the present case, of local variations of the alloy composition. This distribution leads to a broadening of the alloy spectrum lines which is more perceptible for higher velocities (i.e. at both extremities of the alloy spectrum). In order to improve the whole spectrum fitting, the alloy six-line pattern was analyzed, in the following, as a combination of three two-line patterns characterized, each of them, by different line widths. For the other compounds which appeared in the studied samples, all the lines corresponding to a define spectrum were, on the contrary, constrained to have the same width.

Experiments were also carried out to compare the reactivity of the pure metals with those of the iron–cobalt

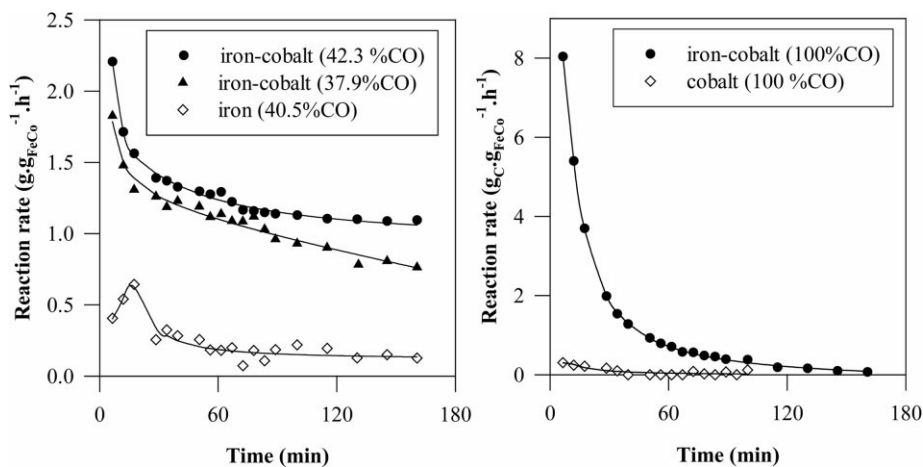


Fig. 3. Comparison of the alloy reactivity with that of its pure components.

mixture. The pure metals catalysts were prepared using the same method as previously described for the iron–cobalt catalyst. The reaction kinetic was shown to differ considerably whether pure metals or an iron–cobalt mixture were used. As can be seen in Fig. 3, lower reaction rates were systematically measured in the case of the pure metals. In addition, these catalysts were shown to be more sensitive to deactivation than the iron cobalt catalyst.

In conclusion, all these results seem to corroborate that iron and cobalt are really alloyed.

#### 4. Evolution of the reaction rate at the beginning of the reaction

The results of our kinetic study demonstrate that the time required to reach the maximal rate decreases when the CO percentage is increased. As an indication, maximal rates were measured at 800 K after times varying from 30 to 60 min for CO percentages lower than 30% and after only 6 min for higher CO percentages.

We will refer in this work to the classical model for the carbon filament growth. According to this model, the carbon-bearing gas adsorbs at the surface of the particle (gas–metal interface) and decomposes. The resulting species dissolve then into the metal particle and diffuse through the particle to the rear faces (metal–carbon interface) where they precipitate to form a filamentous carbon structure. The filament growth is probably initiated at distinct times for each particle depending on parameters like the particle diameter, the crystallographic structure of the surface, etc. The initial increase of the reaction rate would be therefore characteristic of a transient regime.

A model for the evolution of the carbon concentration in a catalyst particle during this initial period is proposed in Fig. 4. This model is deliberately simplistic and has to be considered as a simplified version of the model

proposed by Snoeck et al. [18,19]. Contrary to these authors, we do not take into account the segregation behavior of the carbon, which induces some differences in the carbon concentration profile inside the particle, principally near the surface. We believe, however, that these differences do not question the validity of our reasoning.

The carbon concentration in the particle is expected to considerably increase during the period preceding the carbon nucleation. Since no filament growth is observed, it is, indeed, probable that the carbon issued from the CO decomposition at the surface diffuses through the catalyst particle and accumulates leading to a carbon supersaturation. According to this model, the nucleation occurs when the carbon concentration at the support side exceed a critical value, noted  $C^*$ . As the filament growth is initiated, the carbon concentration at the support side drops to a value equal to the carbon filament solubility in the alloy.

The time required to reach the critical concentration  $C^*$  depends, in this model, on the concentration gradient in the particle. If an equilibrium is established at the gas–metal interface, the carbon concentration at this interface is determined by the composition of the gas mixture and increases as the CO percentage is augmented. It follows that the nucleation occurs more quickly when the CO fraction in the mixture is higher. This is in good agreement with the evolution evidenced experimentally (i.e. the time required to reach the maximal reaction rate decreases as the CO percentage in the gas mixture is increased).

Another phenomenon which frequently occurs at the beginning of the reaction is the fragmentation of the largest catalyst particles into smaller ones. This phenomenon plays a predominant role when the catalyst is used in the form of foils or filings since it is generally assumed that only the smallest particles are active towards filament formation. The fragmentation, as it enlarges the active surface of the catalyst, induces an increase of the reaction rate. The catalyst is,

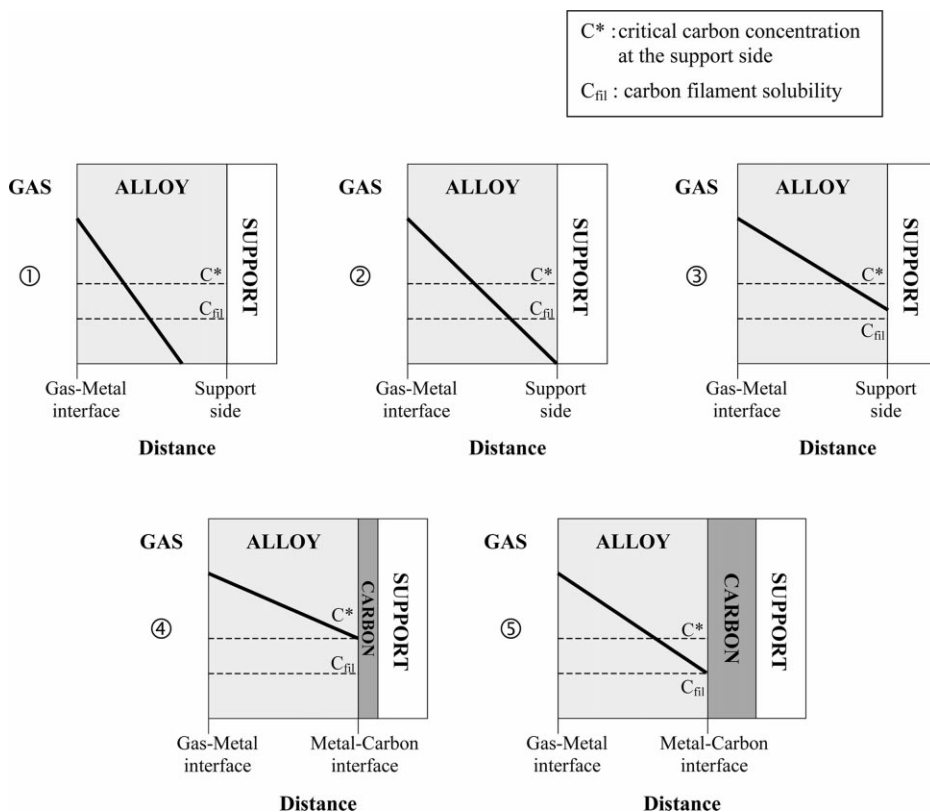


Fig. 4. Evolution of the carbon concentration inside the catalyst particle at the beginning of the reaction. (1), (2), (3): carbon accumulation inside the particle, (4): beginning of the carbon filament nucleation, (5): steady state growth of the carbon filament.

in the present case, supported by a substrate. The catalyst particles are therefore smaller than in the case of catalyst foils or filings and direct reaction of the particles with the gases is possible without preliminary fragmentation. The contribution of fragmentation to the initial increase of the reaction rate can therefore be considered as secondary.

Several authors [20,21] mention the existence of an initial induction period during which no reaction is observed. No such phenomenon was noticed in our case. It seems, on the contrary, that carbon deposition rapidly occurs after the catalyst is contacted with the gas mixture. This fact is supported by T.E.M. observations which clearly establish the filamentous nature of the carbon deposit after a reaction time equal to 15 min (Fig. 5).

## 5. Evolution of the reaction rate after the maximum

The evolution of the reaction rate after the maximum was shown to depend strongly on the composition of the gas mixture. The reaction rate was, indeed, observed either to level off or to decrease steadily depending on the CO percentage. The following study was carried out to identify the processes responsible for the catalyst deactivation.

### 5.1. Stability of the compounds formed during the reaction

A preliminary experiment was carried out to estimate the stability of the compounds formed during the reaction. A catalyst was, first, completely deactivated by reaction with pure CO at 800 K. After the reactor was flushed with helium, the temperature was then rapidly decreased to 293 K. The catalyst was maintained at this temperature for 20 h. After this period, the temperature of the reactor was increased to 800 K and the catalyst was anew contacted with pure CO. No recovery of the catalyst activity was observed after this treatment. This experiment demonstrates that the compounds responsible for the deactivation of the catalyst are stable (or metastable) under inert atmosphere and that they can therefore be isolated using classical analysis techniques.

### 5.2. State of the catalyst after the reaction

The kinetic curves corresponding to a first set of experiments are plotted in Fig. 6. These experiments were conducted until complete deactivation of the catalyst. In some cases (namely with 89.7 and 100%CO), the experiments were pursued even after the reaction had stopped in

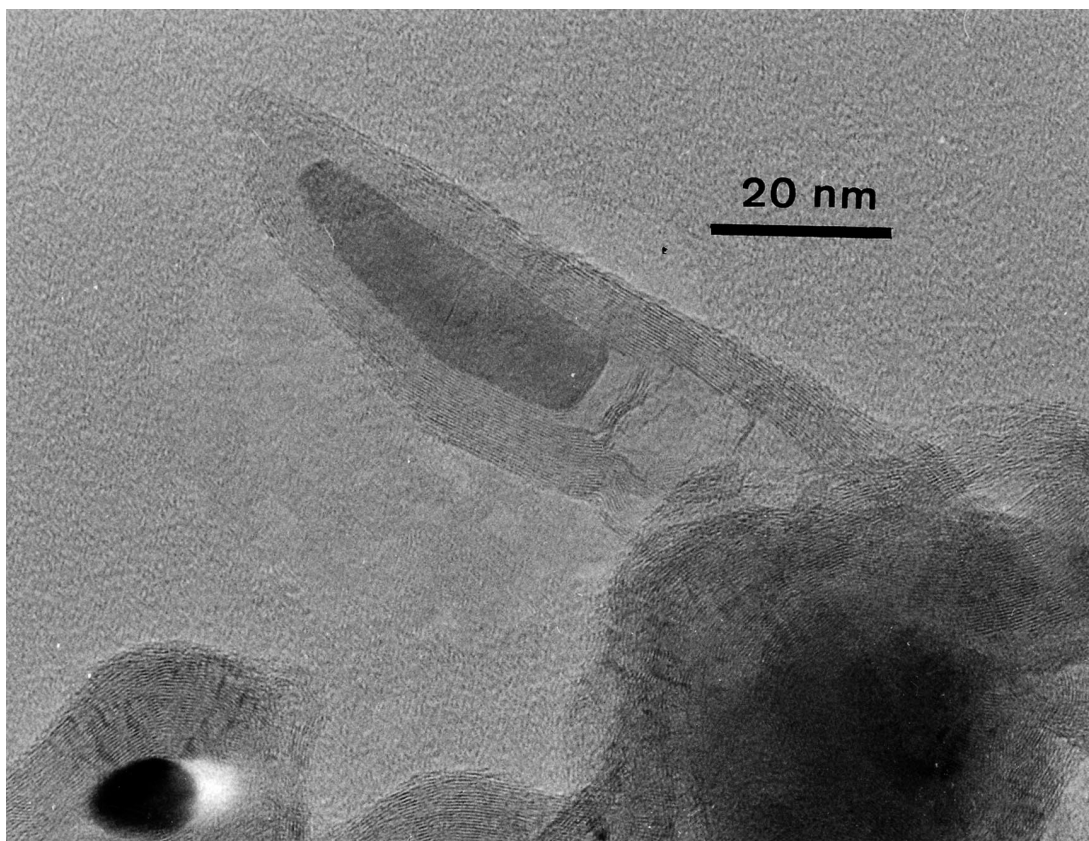


Fig. 5. Carbon filament formed after a 15-min reaction.

order to increase the catalyst transformation. The only exception concerned the reaction with 31.3%CO. The catalyst was, in this case, still active when the experiment was stopped, 23 h after the beginning of the reaction.

The evolution of the different compounds contributions is plotted in Fig. 7 as a function of the gas mixture composition. We define the contribution of a compound as the ratio between the area of its pattern and that of the whole Mössbauer spectrum. As can be seen, the resin contribution is relatively constant and accounts for approximately 6–7% of the total spectrum area. Since it originates from an impurity, the resin contribution constitutes a good gauge of the measures uncertainty. We resolved, for this reason, to only consider as really present the compounds whose contribution exceeded that of the resin.

The presence of magnetite  $\text{Fe}_3\text{O}_4$  was evidenced by Mössbauer spectroscopy for 31.3%CO (Fig. 8). This iron oxide exhibits at room temperature a complex asymmetrical spectrum. The most recognizable absorption lines of this spectrum are located at about  $7.9 \text{ mm}\cdot\text{s}^{-1}$  and between  $-8$  and  $-6.5 \text{ mm}\cdot\text{s}^{-1}$  [22]. The formation of  $\text{Fe}_3\text{O}_4$  was confirmed by X-ray diffraction (Fig. 9). The diffraction pattern of this sample exhibits, indeed, lines for  $2\theta$  values closer from  $35.422$ ,  $56.942$  and  $62.515^\circ$  which are characteristic of

this oxide. As visible on Figs. 8 and 9, the lines corresponding to  $\text{Fe}_3\text{O}_4$  disappear, both on diffraction diagrams and Mössbauer spectra, for higher CO percentages.

The Mössbauer spectra obtained for 89.7 and 100%CO can be described, neglecting the resin contribution, as a combination of two six-line patterns. The first of them is attributable to the alloy. From the number and the position of the absorption lines, the second pattern was ascribed to the cementite  $\theta\text{Fe}_3\text{C}$ .

The iron atoms are distributed in this carbide between two kinds of sites submitted to close hyperfine fields (206 and 208 kOe at 296 K) and having a similar isomeric shift ( $0.18 \text{ mm}\cdot\text{s}^{-1}/\alpha\text{Fe}$  at 296 K) [23]. The atoms occupying these two sites are consequently undiscernible below the Curie temperature ( $T_C = 485 \text{ K}$ ) and the six-line patterns corresponding to each site are completely merged into an unique sextuplet.

$\theta\text{Fe}_3\text{C}$  is not the only iron carbide exhibiting such a spectrum.  $\epsilon'\text{Fe}_{2.2}\text{C}$  is also known to only have one kind of site [24]. However, the hyperfine field of this compound is too different to make confusions possible with cementite ( $H = 173 \text{ kOe}$  for  $\epsilon'\text{Fe}_{2.2}\text{C}$ ).

The analysis of these samples by means of X-ray diffraction did not provide additional information on the catalyst

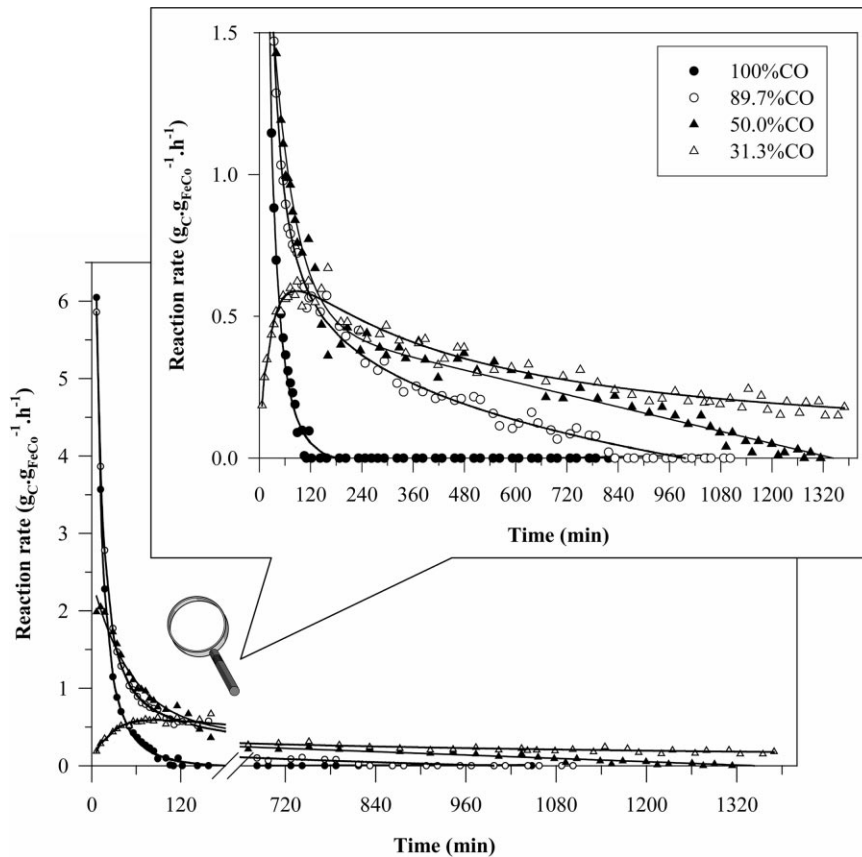


Fig. 6. Time dependence of the reaction rate for different gas mixture compositions (Fe50 Co50 (wt%),  $T = 800$  K).

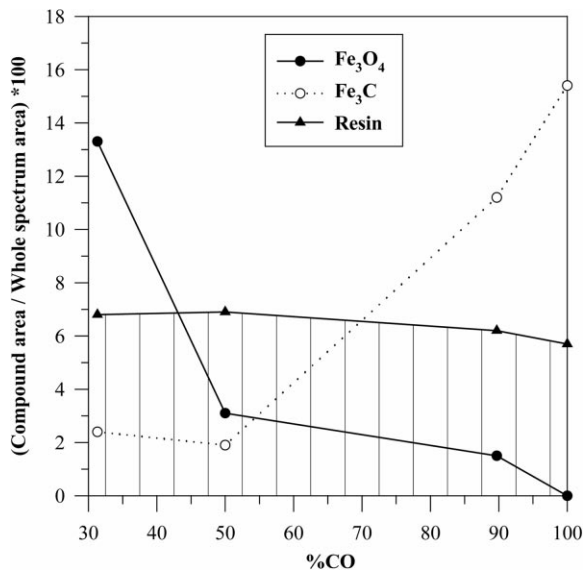


Fig. 7. Evolution of the compounds contributions to the Mössbauer spectrum as a function of the gas mixture composition.

state. No peak attributable either to iron or cobalt carbide was, indeed, clearly evidenced. This result does not question, however, the validity of the Mössbauer analyses. The complexity of the substrate diffraction pattern makes, indeed, difficult the identification of additional peaks. The detection of such peaks is, moreover, complicated by the fact that small amounts of catalysts are generally used (it is to be reminded that the catalyst only accounts for 10% of the weight of the whole sample). In the particular case of the cementite, these difficulties are increased by the fact that the most intense peak corresponding to this carbide is hidden by a peak originating from the alloy.

One of the most important result of this first set concerns the experiment carried out with 50.0%CO. The Mössbauer analysis demonstrated, indeed, that the alloy did not undergo in this case any transformation. This absence of evolution is in accordance with the phase diagram which predicts the existence of an alloy stability domain (Fig. 10). The implications of this result will be discussed further.

Complementary Mössbauer analysis were performed at 77 K. Since temperature variations generally induces great alterations of the spectra appearance, this procedure is often

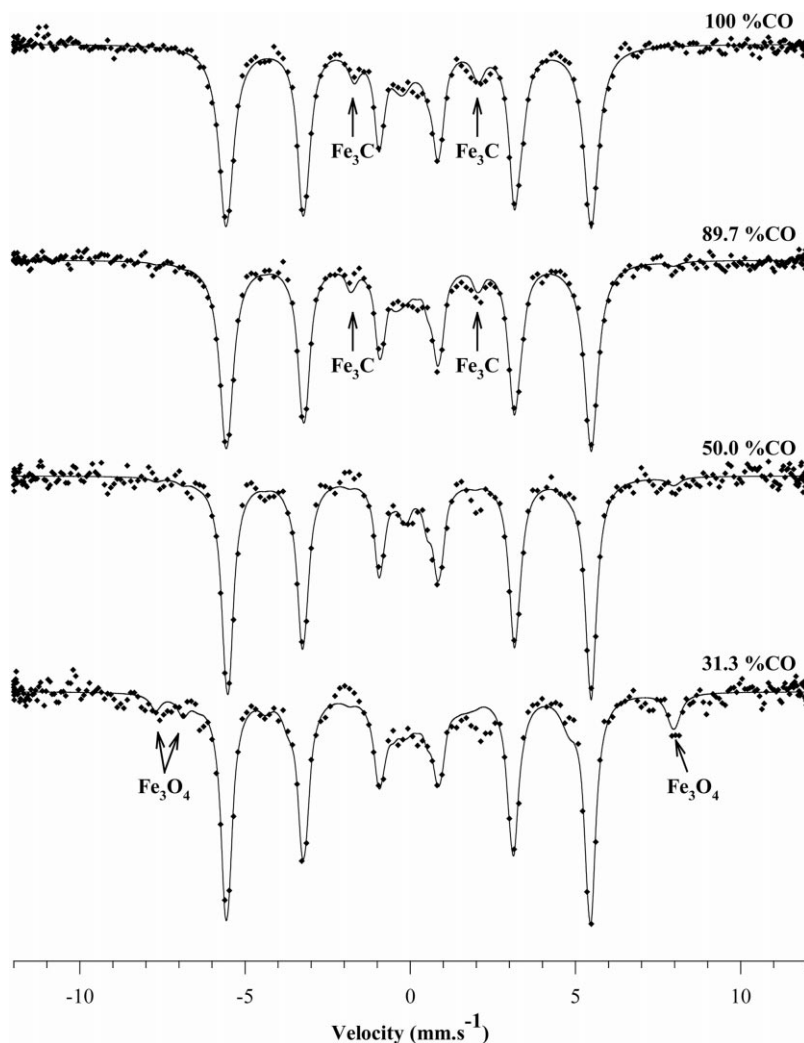


Fig. 8. Evolution of the Mössbauer spectra as a function of the gas mixture composition.

used to confirm the identity of the analyzed compounds. The results of these analyses were close to those obtained at room temperature (Table 1). In particular, the evolution with temperature of the patterns attributed to  $\text{Fe}_3\text{O}_4$  and  $\text{Fe}_3\text{C}$  was shown to agree within the experimental error with that reported in literature.

Fig. 10 illustrates the positioning of the different experiments in the Fe-Co-C-O phase diagram calculated at 800 K. The evolution of the different compounds contributions is, on the whole, in accordance with what was expected from this diagram. Important differences are, however, perceptible respecting the extent of the alloy stability domain.  $\text{Fe}_3\text{O}_4$  was, for example, evidenced for 31.3%CO although the formation of this oxide was not predicted for CO percentages higher than 28%.

Complementary experiments were carried out in order to define more accurately the limits of the alloy stability domain.

The position of these experiments on the phase diagram is illustrated on Fig. 11 and the results are summarized in Fig. 12. This second set of experiments demonstrated that the formation of  $\text{Fe}_3\text{O}_4$  occurred for CO percentages much higher than those predicted (the presence of this iron oxide was, indeed, evidenced for CO percentages as high as 44.6%). On the other hand, the experiment carried out with 57.2%CO seemed to confirm the existence of the alloy stability domain.

Many hypotheses can be proposed to explain the divergences between the experimental results and the predictions of the phase diagram. We favor, for our part, the hypothesis of local variations of the gas mixture composition. The nature of the compounds formed during the reaction depends fundamentally on the CO fraction at the surface of the catalyst particles. Its value may differ notably from the bulk fraction if the reaction is controlled by mass transfer phenomena in the gas phase. Such a phenomenon

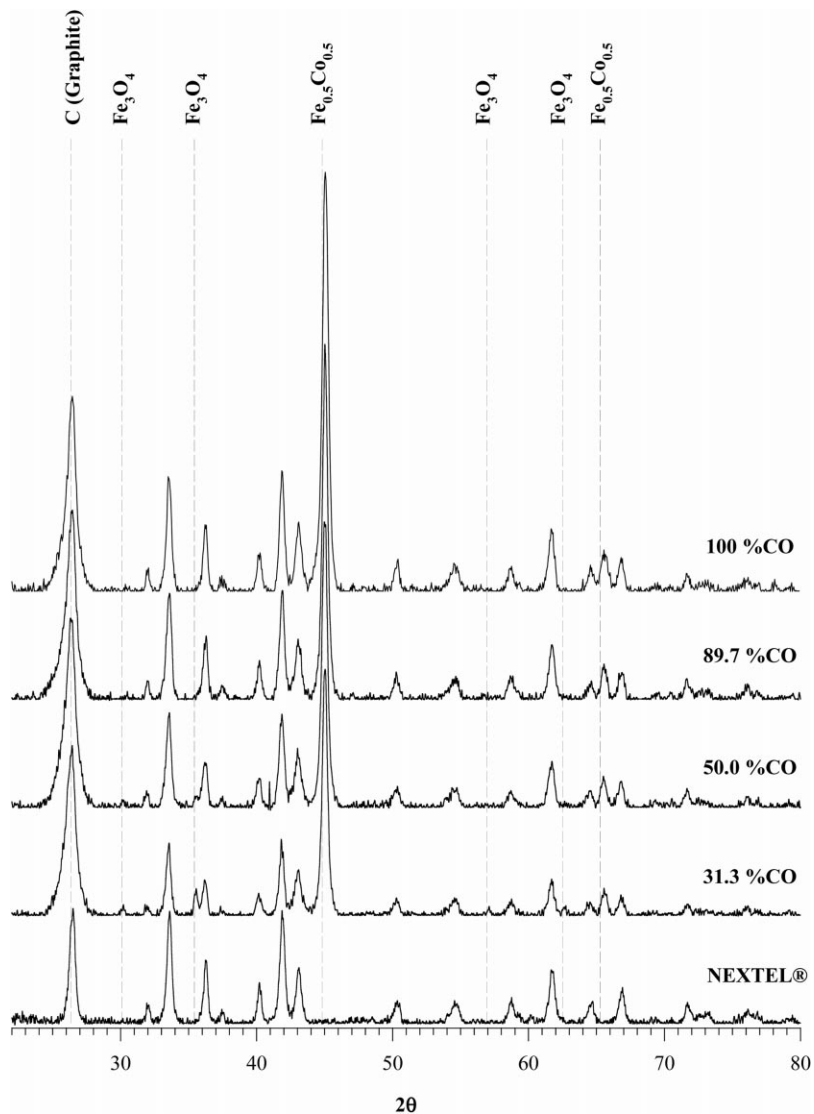


Fig. 9. Evolution of the X-ray patterns as a function of the gas mixture composition.

could explain the displacement of the stability domain observed experimentally. Because of the mass-transfer limitations, the CO percentage of the gas mixture in contact with the particles would, indeed, be lower than that in the bulk and  $\text{Fe}_3\text{O}_4$  could form in apparently unfavorable conditions. It is also within the realm of possibility that the transformations evidenced by Mössbauer spectroscopy and X-ray diffraction for CO percentages higher than 28% do not affect all the particles but only a small fraction of them which would be submitted to local particular conditions.

### 5.3. Evolution of the cobalt during the reaction

The Mössbauer spectroscopy only gives information on

the chemical state of the iron atoms. The reconstitution of the cobalt evolution during reaction was principally based, for this reason, on the information provided by the X-ray diffraction analyses and by the phase diagram. Many parameters made difficult such a study:

- The phase diagrams did not take into account complex compounds (i.e. compounds including both iron and cobalt atoms). The thermodynamic data used to determine the stability domains of the cobalt carbides were moreover doubtful [25].
- The information provided by the X-ray diffraction analyses is not always satisfactory principally for the higher CO percentages.

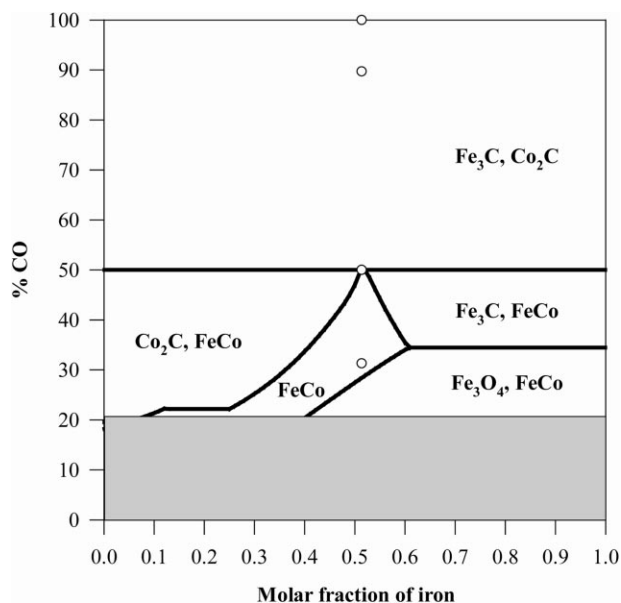


Fig. 10. Position of the first set of experiments at 800 K.

This explains that there was still some doubt on the real state of cobalt after reaction in some cases. The possibility of complex compounds formation, in particular, will be discussed in the following.

CoFe<sub>2</sub>O<sub>4</sub> is, to our knowledge, the only complex oxide reported in literature. As magnetite, CoFe<sub>2</sub>O<sub>4</sub> crystallizes in a face-centered cubic structure. The cell parameters of these two oxides are very close (8.377 Å for CoFe<sub>2</sub>O<sub>4</sub> and 8.396 Å for Fe<sub>3</sub>O<sub>4</sub>). They can hardly, consequently, be differentiated by means of X-ray diffraction.

The Mössbauer analyses enabled, however, in the present case, to rule out the formation of this oxide. The iron atoms

are equally distributed in this oxide between two kinds of sites with similar hyperfine fields (516 kOe) [26]. Ultrafine CoFe<sub>2</sub>O<sub>4</sub> powders are known besides to show superparamagnetic behavior [26,27]. The spectrum of this oxide (a six-line pattern, sometimes superimposed on a two-line pattern) differs greatly, for all these reasons, from the spectrum of magnetite. This result tended to prove the validity of the phase diagram predictions for the lower CO percentages (i.e. only the iron atoms reacted to form Fe<sub>3</sub>O<sub>4</sub> while the cobalt remained unchanged).

In their study of the oxidation of a Ni 59, Fe 41 (wt%) alloy, Greco et al. [28] observed that the interaction of oxygen with a (100) surface induced a pronounced segregation of the alloy components. The compound formed at the surface by reaction with oxygen was predominantly an iron oxide including small amounts of nickel. The nickel ratio could even be reduced by annealing the sample, suggesting that the equilibrium state of this surface oxide corresponded to the pure iron oxide. We can not rule out, in the present case, the occurrence of a similar phenomenon. It is therefore possible that the catalyst particles are covered by a magnetite layer.

For the higher CO percentages, the phase diagram predicts the coexistence of Fe<sub>3</sub>C and Co<sub>2</sub>C. No peak attributable to these compounds was, however, evidenced on the diffraction patterns.

The formation of a complex carbide with a composition close to (Fe<sub>0.5</sub>Co<sub>0.5</sub>)<sub>3</sub>C was reported by Pavel et al. [29] under conditions, however, greatly different from the present ones (these authors were, indeed, interested in synthesizing diamond at a pressure of ~5.5 GPa and a temperature of ~1800 K). On the basis of a Mössbauer study, they

Table 1  
Comparison of the Mössbauer analyses performed at room temperature and 77 K

CO/CO <sub>2</sub> ratio	Contribution to the Mössbauer spectrum (room temperature)	Contribution to the Mössbauer spectrum (77 K)
31.3%CO	Alloy: 77.5% Fe <sub>3</sub> O <sub>4</sub> : 13.3% Fe <sub>3</sub> C: 2.4% Resin: 6.8%	Alloy: 79.5% Fe <sub>3</sub> O <sub>4</sub> : 14.2% Fe <sub>3</sub> C: 0.0% Resin: 6.3%
50.0%CO	Alloy: 88.1% Fe <sub>3</sub> O <sub>4</sub> : 3.1% Fe <sub>3</sub> C: 1.9% Resin: 6.9%	Alloy: 90.4% Fe <sub>3</sub> O <sub>4</sub> : 3.0% Fe <sub>3</sub> C: 0.0% Resin: 6.6%
100%CO	Alloy: 78.9% Fe <sub>3</sub> O <sub>4</sub> : 0.0% Fe <sub>3</sub> C: 15.4% Resin: 5.7%	Alloy: 84.0% Fe <sub>3</sub> O <sub>4</sub> : 0.0% Fe <sub>3</sub> C: 10.2% Resin: 5.8%

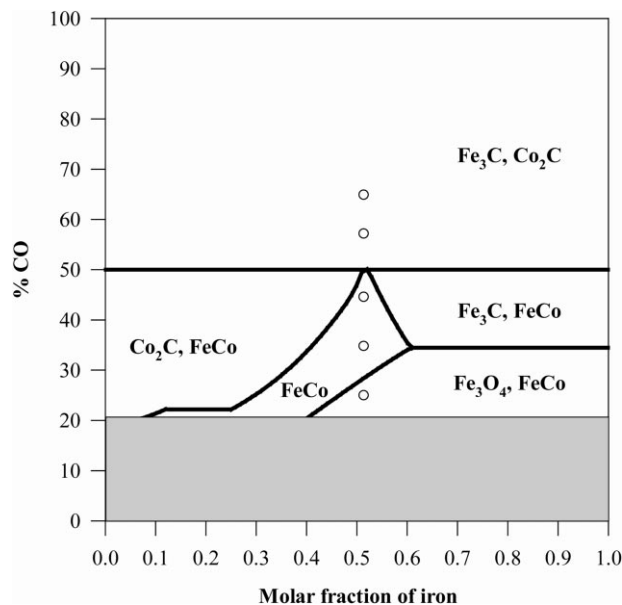


Fig. 11. Position of the second set of experiments at 800 K.

attributed to this carbide an hyperfine field of 193.5 kOe, value which is slightly lower than that of cementite (206,208 kOe).

This complex carbide would be structurally equivalent to a solid solution of  $\text{Fe}_3\text{C}$  and  $\text{Co}_3\text{C}$ . These two compounds have a similar crystallographic structure and very close cell unit parameters (Table 2). The formation of a solid solution involving these two compounds is therefore fully plausible.

(It must be noted that a similar reasoning with  $\text{Fe}_3\text{C}$  and  $\text{Co}_2\text{C}$  brings us to the conclusion that these two phases are, on the contrary, not miscible). As no thermodynamic data concerning this complex carbide was available, the determination of the conditions favoring its formation was not possible. The positioning of its stability domain in the phase diagram is, therefore, still a mystery.

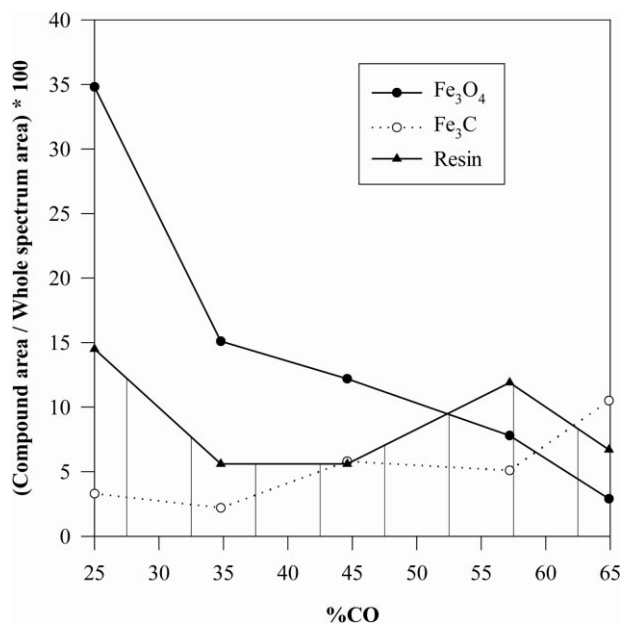


Fig. 12. Evolution of the compounds contributions to the Mössbauer spectra as a function of the gas mixture composition (second set of experiments).

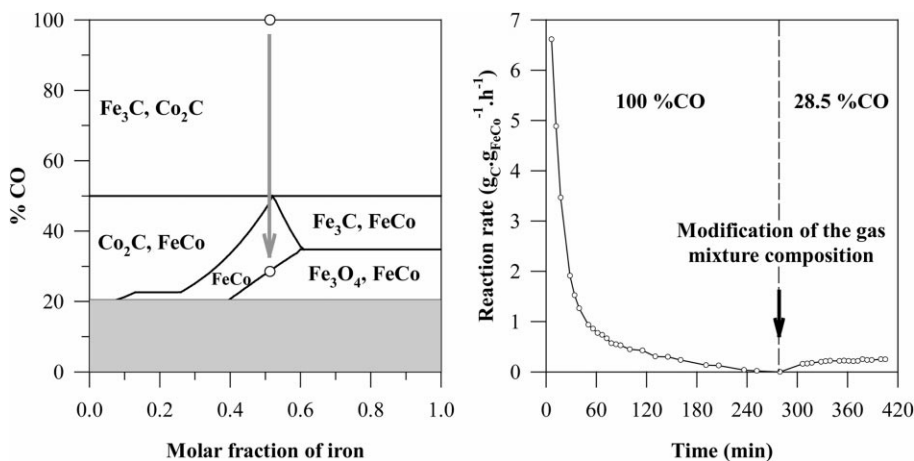


Fig. 13. Influence of a modification of the gas mixture composition on the reaction rate.

Failing more accurate information, no definitive conclusion can be drawn concerning the state of cobalt for the higher CO percentages. Cobalt could either exist as  $\text{Co}_2\text{C}$  (as predicted by the phase diagram) or form as  $\text{Co}_3\text{C}$  a solid solution with  $\text{Fe}_3\text{C}$ . As previously the hypothesis of a segregation of the alloy components cannot be ruled out. The surface of the particles could therefore be covered by a  $\text{Fe}_3\text{C}$  layer.

## 6. Deactivation mechanism of the alloy

It appears from this study that the formation of  $\text{Fe}_3\text{O}_4$  only slightly affects the reaction rate. This result can be interpreted in two different ways:

1. The magnetite catalytic activity is similar to that of the iron cobalt alloy. Bennet et al. [30] have managed to obtain carbon filaments by reacting  $\text{Fe}_3\text{O}_4$  with acetone. The few information we have about these experiments does not permit, however, to conclude whether  $\text{Fe}_3\text{O}_4$  is really the active phase or it is reduced when contacted with acetone (which would mean that the decomposition of acetone is, in fact, catalyzed by iron).
2. The magnetite has no catalytic activity but its formation leads to a fragmentation of the catalyst particles. The resultant increase of the active area could therefore compensate the fact that  $\text{Fe}_3\text{O}_4$  does not catalyze the CO disproportionation.

The results of this study also demonstrate a strong implication of cementite (may be in association with a cobalt carbide) in the alloy deactivation process. A survey of the kinetic results shows, indeed, that the catalyst deactivation occurs all the more rapidly that the CO ratio in the gas mixture is higher. As demonstrated by the Mössbauer analyses, this evolution can be correlated to an increase of the  $\text{Fe}_3\text{C}$  amount formed during the reaction.

In order to confirm this hypothesis, we submitted, in the same experiment, a reduced catalyst to gas mixtures with different CO/ $\text{CO}_2$  ratios (Fig. 13). The catalyst was, first, contacted with pure CO at 800 K. In accordance with the phase diagram which predicts that such conditions favor the formation of the carbide phases, a complete deactivation of the catalyst was observed 3 h after the beginning of the reaction. The composition of the gas mixture was, at this time, rapidly modified (28.5%CO) in such a way that the catalyst was submitted to conditions under which the carbide formation was not thermodynamically possible. A recovery of the catalyst activity was, then, rapidly observed. This experiment, as well as it confirmed the role played by the carbide phases in the poisoning process, demonstrated that the alloy deactivation is (at least partially) a reversible phenomenon. It is noteworthy that the evolution of the reaction rate after the catalyst activity recovery was similar to that previously described for the lower CO percentages. The reaction could be, indeed, prolonged for 16 h after the modification of the gas mixture composition and no

Table 2  
Crystallographic structure of  $\text{Fe}_3\text{C}$  and  $\text{Co}_3\text{C}$

Compound	Structure	Cell parameters (Å)		
$\text{Fe}_3\text{C}$	Orthorhombic	$a = 5.0910$	$b = 6.7434$	$c = 4.5260$
$\text{Co}_3\text{C}$	Orthorhombic	$b = 4.993$	$c = 6.707$	$a = 4.444$

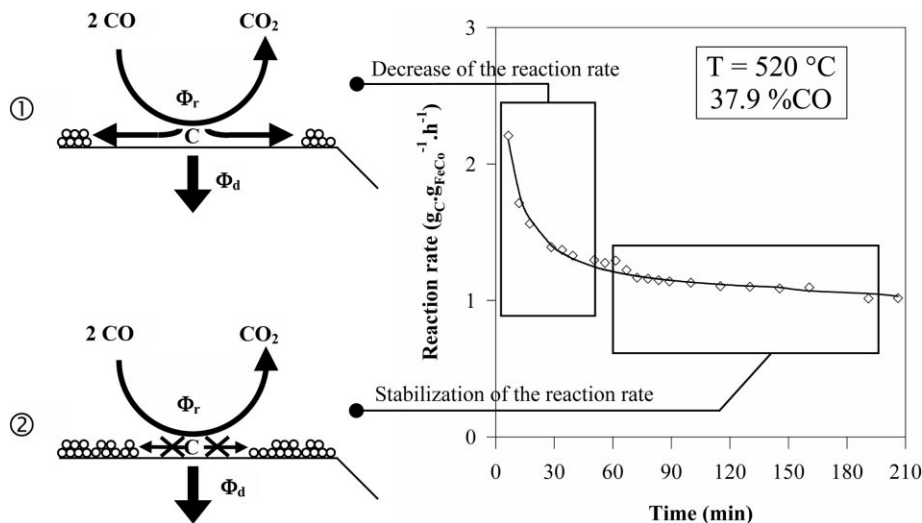


Fig. 14. Alloy deactivation mechanism when the carbide formation is not thermodynamically possible. 1.  $\Phi_r > \Phi_d$ : formation of a carbon layer at the surface of the particle. 2.  $\Phi_r = \Phi_d$ : the carbon coating stops.

sign of catalyst deactivation was perceptible when the experiment was stopped.

We can conclude on the basis of these results that the cobalt and iron carbides have no catalytic activity towards the carbon monoxide disproportionation. Concerning the cementite, this conclusion is consistent with the findings of authors who have studied the interactions between iron and carbon-bearing gases [31–33].

This study demonstrates, however, that the carbide formation is not the only phenomenon responsible for the catalyst poisoning. The Mössbauer analyses performed for 50.0 and 57.2%CO showed, indeed, that the deactivation did not result from a chemical transformation of the catalyst. In the absence of any chemical transformation of the catalyst, the most probable hypothesis is that the deactivation results, in this case, from the formation of a carbon layer at the surface of the particles which will prevent any contact with the gas mixture.

According to our experimental results, the carbon coating would only occur at 800 K for CO percentages higher than 35–45%. At the same temperature, the carbide formation was only evidenced for CO percentages higher than 57–65%. The number of interfering phenomena would, therefore, depend on the gas mixture composition. This would explain the different evolutions of the reaction kinetics with the composition of the gas mixture.

It can be assumed that the carbon coating occurs when the rate of carbon produced by the CO disproportionation at the surface (noted  $\Phi_r$ ) is greater than the rate diffusing through the particle ( $\Phi_d$ ). A model for the catalyst deactivation when no carbide formation is thermodynamically possible is proposed in Fig. 14. The formation at the beginning of the reaction of a carbon layer partially isolating the surface of the particles from the gas phase leads to a important

decrease of the reaction rate (figure). The rate of carbon produced at the surface becomes, for this reason, progressively closer to that diffusing through the alloy particle. When the equality is reached, the carbon coating stops and the reaction rate stabilizes at a constant value. In absence of other deactivating phenomenon, no further decrease of the reaction rate should be observed. Our results seems to demonstrate, however, that the carbon coating goes on, with a reduced rate, until complete deactivation of the catalyst. This idealized model has the merit of explaining the initial decrease of the reaction rate as well as its posterior stabilization.

The previous model is slightly modified when the carbide formation becomes thermodynamically possible (Fig. 15). The deactivation of the catalyst is, in that case, the consequence of two phenomena acting conjointly. As previously, the carbon coating and the carburization of the catalyst particles leads to a strong decrease of the reaction rate in the beginning of the reaction. When  $\Phi_r$  becomes equal to  $\Phi_d$ , the carbon coating phenomenon is stopped (or, at least, notably slowed down). The carbide formation proceeds, on the contrary, until complete transformation of the particles surface. No stabilization of the reaction rate is, therefore, observed in this case and the carbide formation on the carbon-free surface leads rapidly to complete deactivation of the catalyst. A good example of such an evolution is given by the experiment carried out under pure CO.

## 7. Conclusion

The formation of cementite  $\text{Fe}_3\text{C}$  was evidenced at 800 K by Mössbauer spectroscopy for CO percentages higher than 57–65%. The results of this study demonstrate that this

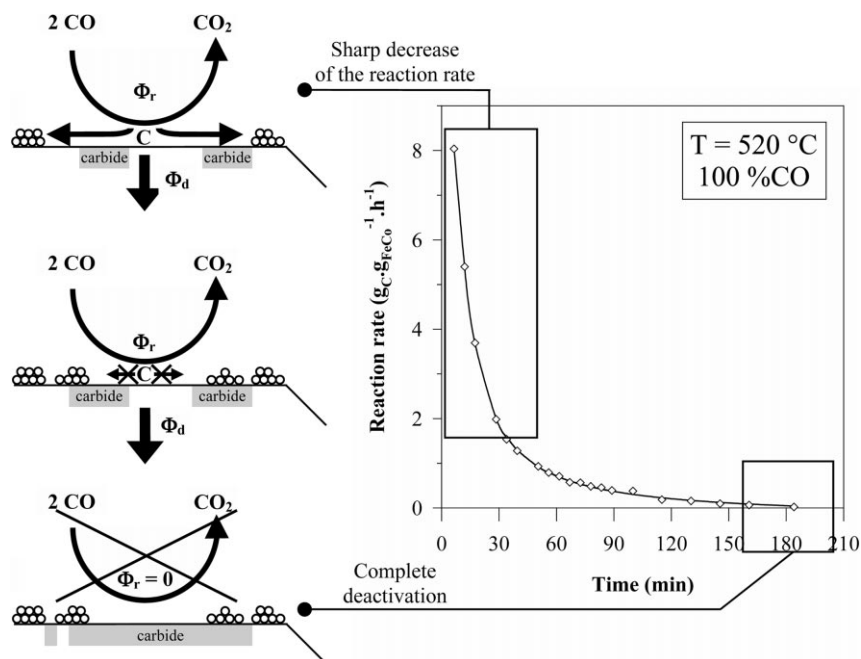


Fig. 15. Alloy deactivation mechanism when the carbide formation is thermodynamically possible. 1.  $\Phi_r > \Phi_d$ : carbide formation + carbon coating. 2.  $\Phi_r = \Phi_d$ : the carbon coating stops but the carbide formation goes on. 3. The carbon-free surface is completely carburized.

compound is strongly involved in the alloy deactivation phenomenon. The catalyst was, indeed, shown to partially recover its activity when submitted to conditions under which the carbide formation was not thermodynamically possible.

The results of this study seem to indicate, however, that the alloy deactivation is not the consequence of a single phenomenon but results from the conjunction of two distinct processes. The alloy deactivation for 50.0%CO was, indeed, found not be due to any chemical transformation. Additional deactivation due to the formation of a carbon layer at the particles surface appears as the most plausible hypothesis to explain this result.

The evolution of the cobalt atoms during the reaction was not clearly elucidated. Contrary to the predictions of the Fe-Co-C-O diagrams, no cobalt carbide could be evidenced by means of X-ray diffraction. Its formation is nevertheless plausible. A segregation of the two alloy components during the reaction can not be ruled out.

## References

- [1] M. Audier, J. Guinot, M. Coulon, L. Bonnetain, Carbon 19 (1981) 99.
- [2] S. Herreyre, P. Gabelle and J.L. Ginoux, in Extended Abstracts Carbon '94, Granada, Spain, 5222 (1994).
- [3] P.E. Nolan, M.J. Schabel, D.C. Lynch, A.H. Cutler, Carbon 33 (1995) 79.
- [4] J.H. Hafner, M.J. Bronikowski, B.R. Azamian, P. Nikolaev, A.G. Rinzler, D.T. Colbert, K.A. Smith, R.E. Smalley, Chem. Phys. Letters 296 (1998) 195.
- [5] A. Thaib, G.A. Martin, J.P. Pinheiro, M.C. Schouler, P. Gabelle, Catal. Lett. 63 (1999) 135.
- [6] N.M. Rodriguez, A. Chambers, R.T.K. Baker, Langmuir 11 (1995) 3862.
- [7] P.E. Nolan, D.C. Lynch, A.H. Cutler, J. Phys. Chem. B102 (1998) 4165.
- [8] J.P. Pinheiro, M.C. Schouler, P. Gabelle, M. Mermoux, E. Doorhyee, Carbon 38 (2000) 1469.
- [9] A. Chambers, N.M. Rodriguez, T.K. Baker, J. Phys. Chem. 99 (1995) 10581.
- [10] J.P. Pinheiro and P. Gabelle, J. Phys. Chem. Solids (Accepted for publication).
- [11] J.M. Alameda, D. Givord, C. Jeandey, H.S. Li, Q. Lu, J.L. Oddou, J. Physique 46 (1985) 1581.
- [12] S. Herreyre, Thesis, Grenoble, 1995.
- [13] W.C. Ellis, E.S. Greiner, Tr. Amer. Soc. Met. 29 (1941) 415.
- [14] W.B. Pearson, in Handbook of Lattice Spacings and Structures of Metals and Alloys. Edited by Pergamon Press Ltd, London, Great Britain, 1964.
- [15] F.W.C. Boswell, Proc. Phys. Soc. A 64 (1951) 465.
- [16] E.A. Owen, D. Madoc Jones, Proc. Phys. Soc. B 67 (1954) 456.
- [17] C.E. Johnson, M.S. Ridout, T.E. Cranshaw, P.E. Madsen, Phys. Rev. Letters 6 (9) (1961) 450.
- [18] J.-W. Snoeck, G.F. Froment, M. Fowles, J. Catal. 169 (1997) 240.
- [19] J.W. Snoeck, G.F. Froment, M. Fowles, J. Catal. 169 (1997) 250.
- [20] F.W.A.H. Geurts, R.G. Cnossen, A. Sacco Jr., R.R. Biederman, Carbon 32 (1994) 1151.

- [21] C. Vanvoren, Thesis, Grenoble, 1981.
- [22] L. Haggström, H. Annersten, T. Ericsson, R. Wäppling, W. Karner, S. Bjarman, *Hyperfine Interactions* 5 (1978) 201.
- [23] G. Le Caër, J.M. Dubois, J.P. Senateur, *J. Solid State Chem.* 19 (1976) 19.
- [24] J.W. Niemantsverdriet, A.M. van der Kraan, W.L. van Dijk, H.S. van der Baan, *J. Phys. Chem.* 84 (1980) 3363.
- [25] Cobalt Monograph Edited by Centre d'Information du Cobalt, 1960.
- [26] T.K. McNab, A.J.F. Boyle, Proceedings of the Conference on Hyperfine Structure and Nuclear Radiations, North Holland, Amsterdam, 1968, p. 957.
- [27] W.J. Schuele, S. Shtrikman, D. Treves, *J. Appl. Phys.* 36 (1965) 1010.
- [28] S.E. Greco, J.P. Roux, J.M. Blakely, *Surf. Sci.* 120 (1982) 203.
- [29] E. Pavel, G. Baluta, D. Barb, D.P. Lazar, M. Morariu, M. Popescu, M. Sorescu, *J. Mat. Sci.* 28 (1993) 1645.
- [30] M.J. Bennet, G.H. Chaffey, A.J. Langford, D.R.V. Silvester, A.E.R.E. Report R7407 (quoted by Ref. [31]).
- [31] R.T.K. Baker, J.R. Alonzo, J.A. Dumesic, D.J.C. Yates, *J. Catal.* 77 (1982) 74.
- [32] P.L. Walker Jr., J.L. Rakszewski, G.R. Imperial, *J. Phys. Chem.* 63 (1959) 140.
- [33] S. Herreyre, P. Gadelle, P. Moral, J.M.M. Millet, *J. Phys. Chem. Solids* 58 (1997) 1539.